IEEE Access
Multidisciplinary | Rapid Review | Open Access Journal

Received December 27, 2019, accepted January 25, 2020, date of publication February 4, 2020, date of current version February 13, 2020.

Digital Object Identifier 10.1109/ACCESS.2020.2971606

Design of Compact mm-wave Tunable Filtenna Using Capacitor Loaded Trapezoid Slots in Ground Plane for 5G Router Applications

KORANY R. MAHMOUD[1,2] AND AHMED M. MONTASER[3]

[1]Department of Electronics and Communications, Faculty of Engineering, Helwan University, Cairo 11795, Egypt
[2]National Telecommunications Regulatory Authority, Ministry of Communication and Information Technology, Giza 12577, Egypt
[3]Electrical Engineering Department, Sohag University, Sohag 82515, Egypt

Corresponding author: Korany R. Mahmoud (kurany_hameda@h-eng.helwan.edu.eg)

This work was supported in part by the National Telecommunication Regulatory Authority (NTRA), Ministry of Communication and Information Technology, Egypt.

ABSTRACT This paper introduces a compact millimeter-wave tunable filtenna with defected ground-plane structure (DGS) resonators for future fifth generation (5G) applications. An approach of adding the lumped and tunable elements within the DGS resonating structure is introduced. The designed filtenna has achieved a good reflection coefficient $|S_{11}|$ lower than -25 dB with a realized gain higher than 9 dB at any of the tuned frequency bands. A good agreement is achieved between the measurements and the simulated results those produced from both the finite difference time domain method (FDTD) Matlab coded and the CST-MWS simulation program. Furthermore, a circular array consists of 16 antenna elements is designed to be integrated into 5G router device. Different scenarios have been considered to show the array performance capability to maximize the array directionality in certain directions at certain frequency and in other directions with another frequency band. Finally, the scan pattern with the coverage efficiency are presented to illustrate the capability of the designed array as a key piece of future 5G routers.

INDEX TERMS Filtenna, bandpass filter, tunable antennas, multi-polarized antenna, beamforming, optimization techniques, mm-wave 5G router.

I. INTRODUCTION

Recently, the inevitable fifth generation (5G) wireless standard will turn into a business reality, however customers and businesses are looking forward the exhibition potential - especially as it will have stamped itself in internet speed. Whereas, downloading such content as games, high- resolution 4K video, and other intensive files will happen mystically quick [1]. Therefore, early prototype 5G routers are coming into shape as the 5G reality be approached. In 2018, Huawei introduced the world's first 3GPP 5G router for the mm-wave frequency range between 26 and 28 GHz which could reach download speed up to 2Gbps [2]. Furthermore, Samsung's first 5G home router has officially won FCC approval ahead of Verizon's 2018 launch [3]. Samsung's FCC grant of approval confirms that the device includes 64 antennas across a beamforming 2×2 MIMO array, including 27.5 GHz to 28.35 GHz millimeter-wave (mm-wave) support. Generally, different service providers such as AT&T and Verizon commenced testing 5G routers for homes and businesses. The resulting performance is giving the market a genuine taste of the speeds to come. Generally, the filtering antenna (filtenna) plays a crucial role in regulating communication systems because it has many features over common antennas such as it eliminates unwanted signals outside the operational range. Therefore, a lot of attention has been paid recently to tunable antennas owing to their capability of tuning the resonance frequency without affecting on the antenna radiation characteristics [4]. One of the possible filtenna structures, is to design the antenna and filter in a cascaded structure. As a result, researchers have investigated a variety of approaches, such as employing stubs [5] split-ring resonators [6] and applying slots, or using capacitive loops [7]. However, in such case, the filtennas are more complex, bigger in sizes, and have higher costs. Besides, the rejection value and sharpness of the achieved band-notch are not satisfied enough. Therefore, the co-designed structure by integrating the antenna with reconfigurable filter is recommended [8]. This structure,

The associate editor coordinating the review of this manuscript and approving it for publication was Akram Alomainy.

as well as being more compact, it reduces the interconnection losses that occur due to cascading the filtering and radiating element in the processing layer [9]. In such case, the filter is usually integrated within the antenna ground plane or in its feeding line. Different filtennas designs have been reported in literatures [10]–[13], but at lower frequencies with either high loss transmission lines or complex constructions. To the best of our knowledge, a little work has been published on the design of mm-wave filtenna design. Although, mm-wave filtenna is one of the most significant component in the design of 5G router to have the merits of high performance, easy integration and low cost. In [14], an integrated design of the filtenna based on substrate integrated waveguide (SIW) technology at 37–38 GHz is presented for local-multipoint-distribution system.

To realize compact size, high performance, and low cost, defected ground-plane structure (DGS) has been broadly used and thoroughly investigated in different mm-wave/ microwave designs and applications in order to go along with the required transmission specifications [15]. In [16], a compact two-layer band stop filter using a DGS resonator is studied with a parasitic stub. Mahmoud and Montaser [17], have considered DGS cell (consists of coupled c-shaped in the ground plane) to enhance the antenna array radiation characteristics operating in mm-wave frequency band from 28 GHz to 38 GHz. However, in all previous investigations, the DGS filtennas are not combined with tunable or lumped elements, they are only used to improve the response of the designed elements.

On the other hand, reconfigurable antennas represent a potential candidate to satisfy the 5G prerequisites [18]–[21]. Varieties of reconfigurable and tunable antennas have been reported [22], [23]. In [22], the filtenna tunability has been achieved by loading the H-shaped resonator with a single varactor from 3.85 to 5.58 GHz. However, Alves *et al.* [23] have developed a frequency-tunable horn filtennas for mm-wave from 17.4 to 24 GHz based on the integration of a broadband horn antenna with a dual-post tunable resonator filter. Undoubtedly, the combination of resonating slots and lumped elements will have an influence on the filtenna performance.

In this paper, we firstly present the design of a novel tunable mm-wave bandpass filter (BPF). Then, the structure of mm-wave filtenna composed of a dual reverse split trapezoid slots DGS resonators located on the truncated ground plane is introduced. For filtenna tunability, lumped capacitor elements have been added within the DGS resonating structure. Finally, a circular array consists of 16 antenna elements is designed to be integrated into 5G router device. In this target, the filtenna design is analyzed completely using the commercially available CST-Microwave Studio software (MWS) package linked with Matlab coded optimization program. Whereas, a recent hybrid approach involving the enhanced central force optimization (ECFO) as a global algorithm and Nelder–Mead (NM) algorithm as a local one [17], [24] is considered to optimize the filtenna dimensions and synthesize the antenna array beam patterns.

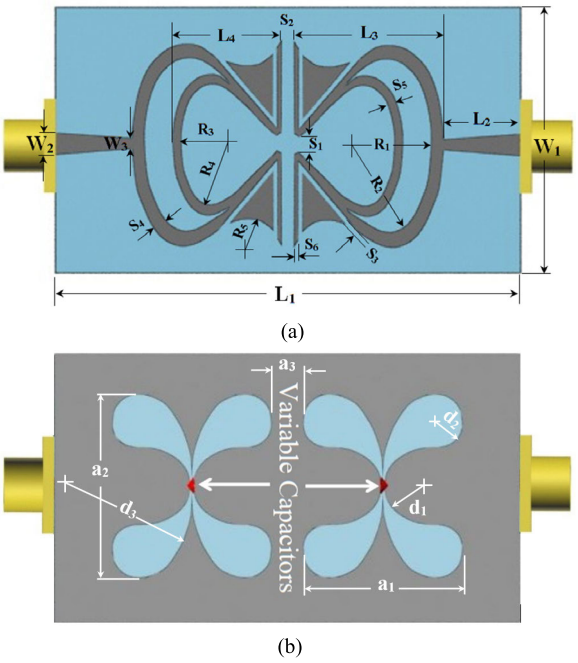

FIGURE 1. Configuration of the proposed BPF. (a) Front view and (b) Back view.

The organization of the present paper is as follows: In Section 2, the design and configuration of BPF, tunable filtenna, and 5G mm-wave router device are introduced. The results and discussions are investigated in Section 3. Finally, Section 4 presents the conclusions.

II. DESIGNS AND CONFIGURATIONS

In this section, the design configuration of the proposed compact BPF, filtenna, and tunable filtenna is introduced. Then, the geometrical configuration of the array consisting of 32-antenna elements embedded into practical router case is described.

A. FILTER CONFIGURATION

The proposed BPF is designed with a mid-band frequency of 28 GHz. It is inductively coupled to the source and is excited via port 1 and port 2 with a 50 Ω feed line. As illustrated in Fig. 1, the BPF is symmetric along the longitudinal and latitudinal axis. The filter consists mainly of a microstrip feed that is integrated with two overlapping ohm Ω figures and were oriented with their gaps face-to-face. The configuration in such case produces an electrical coupling between the two elements (each overlapping ohm Ω figure is consider as one element). Two units of DGS cells are etched in the truncated ground in bottom as shown in Fig. 1b, each one consists of x-like shape.

The structure is designed on a Rogers RT5880 substrate of a 0.508 mm thickness, having a dielectric permittivity of $\varepsilon_r = 2.2$, loss tangent of 0.0009. The modelling simulations of the proposed filter were done using the commercially available software CST Microwave Studio and also simulated

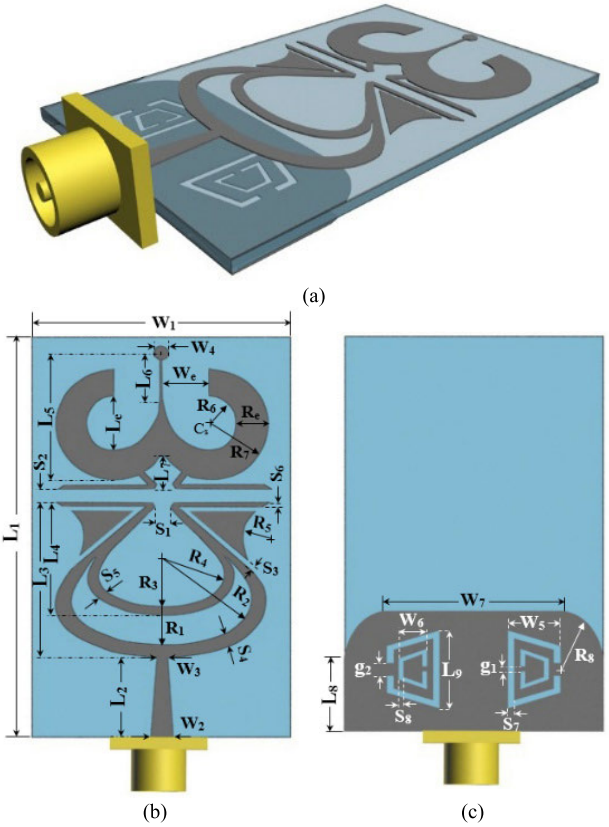

FIGURE 2. Configuration of proposed filtenna design. (a) 3D metal pattern, (b) Front view and (c) Back view.

using the FDTD method written in Matlab code. In addition, the simulation results were compared with the measurements.

B. TUNABLE FILTENNA DESIGN CONFIGURATION

The proposed tunable filtenna will be presented based on the optimized tunable BP filter considering partial ground plane with x-shaped DGS slots. The 3D design configuration of the proposed compact tunable filtenna is illustrated in Fig. 2a. The design is excited via SMA port with a 50-Ω feed line. The filtenna is composed of two radiation elements: the patch and the truncated ground plane. As shown in Fig. 2b, the patch consists of two overlapping omega Ω figures oriented with their gaps face-to-face with tapered annular part of 3-like shape. Two unit DGS cells are etched in the truncated ground in bottom of filtenna as shown in Fig. 2c, each one consists of a dual reverse split trapezoid slots. Similar to the strip-type of split ring resonator (SRR), these DGS cells provide high Q-characteristic. To provide more coupling with the field, the etched cells were located near the feeding line. For tuning the frequency band, the variable capacitor will be placed in the middle of the largest side of the trapezoid truncated in the ground plane.

C. FILTENNA ARRAY FOR mm-wave 5G ROUTER

In this work, a circular array antenna geometry is introduced as shown in Fig. 3a. The array consists of 16 circularly

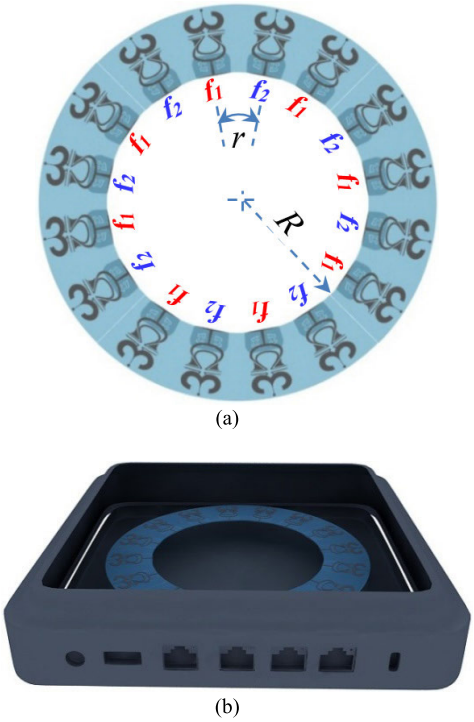

FIGURE 3. Configuration of the proposed 5G mm-wave router. (a) Filtenna array geometry and (b) 3D router structure.

polarized antenna elements. The elements are uniformly distributed in a circle configuration with a ring radius $R = 10\lambda$, with center-to-center distance (r) of approximately 4.2λ, where λ is the wavelength of 28 GHz. Then, the array is packed with a dielectric plastic material of relative permittivity $= 4.5$ and conductivity $\sigma = 0.0004$ S/m.

The proposed 5G mm-wave router is designed to synthesize the beam-patterns adopting polarization and directivity control with two different frequencies simultaneously. On other words, the array is required to direct V/H multi-beam patterns towards the dedicated users while placing deeper nulls towards the interferer directions with different frequencies simultaneously. In such case, half of the array elements (odd elements) will be resonated at the f_1 and the others (even elements) will operate at f_2 by tuning the capacitance lumped elements as shown in Fig 3a. Thus, the antenna element phases will be optimized, whereas, the phases are allowed to vary between $-\pi$ to $+\pi$, respectively.

III. NUMERICAL SIMULATIONS AND MEASUREMENTS

In this section, the simulations and measured results of the optimized BPF, filtenna, and tunable filtenna will be firstly presented, analyzed and compared. Consequently, the simulation results of the designed mm-wave 5G router will be introduced showing their beamforming capabilities with different scenarios. Furthermore, the performance of the proposed 5G router is illuminated using the metrics of total scan pattern and coverage efficiency.

TABLE 1. The bandpass filter optimized dimensions (in millimeter).

Variable	Initial value	Decision space		Best value
		from	to	
L_1	-	-	-	15
L_2	2	2	3.5	2.26
L_3	3	3	5	4.25
L_4	2.5	2.5	4	3.13
W_1	-	-	-	7.5
W_2	0.5	0.5	1	0.75
W_3	0.3	0.3	0.5	0.41
S_1	0.25	0.25	1	0.51
S_2	0.2	0.2	0.8	0.45
S_3	-	-	-	0.2
S_4	0.25	0.25	0.75	0.51
S_5	0.15	0.15	0.35	0.25
S_6	0.1	0.1	0.3	0.19
R_1	1.5	1.5	3	2.25
R_2	2.5	2.5	3	2.75
R_3	1	1	1.5	1.43
R_4	1.5	1.5	2	1.75
R_5	-	-	-	1
a_1	4.5	4	5.5	5.1
a_2	4.5	4	5.5	5.09
a_3	1.5	0.5	3	1
d_1	1.25	1	1.5	1.12
d_2	1.25	1	1.5	0.91
d_3	3.5	3	4.5	4.1

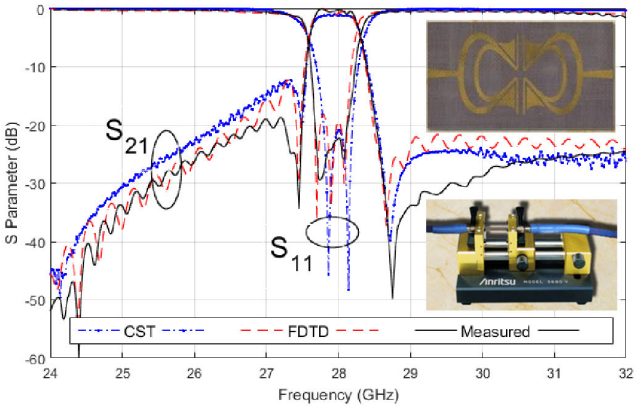

FIGURE 4. S-parameters of the proposed bandpass filter.

A. FILTER PERFORMANCE RESULTS

The proposed BPF is completely designed by simulating the filter using CST-MWS linked to the Matlab compiler to optimize the filter dimensions based on the ECFO-NM algorithm. Accordingly, the applied objective function has focused on minimizing the filter return loss (S_{11}) and maximizing the insertion loss (S_{21}) at the required operating frequency band of 28 GHz as in Eq. (1):

$$Obj_1 = \{min[S_{11}(f)] + max\,[S_{21}(f)]\}_{f=28GHz} \quad (1)$$

The optimized dimensions including the assigned decision space are listed in Table 1. Fig. 4 shows a comparison between the measured data and simulation results either using CST-MWS or FDTD of the return loss S_{11} and insertion loss S_{21}. A photograph of the fabricated BPF and test fixture are inset into the Figure. It is can be observed that return loss is −22.29, −20.95, −19.24 dB at 28 GHz for measured,

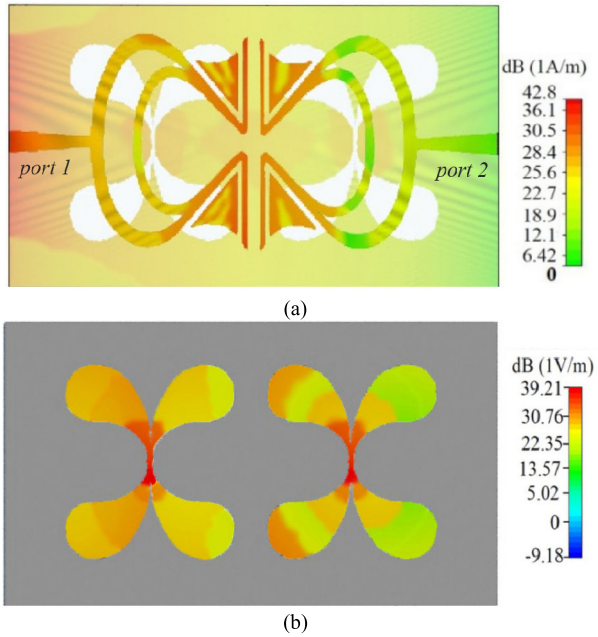

FIGURE 5. Simulated current and voltage distribution of the optimized BPF. (a) Current distribution on top layer and (b) Electric field intensity on etched *x* -shaped DGS.

simulated using CST-MWS software package and FDTD Matlab code, respectively. Besides, the obtained insertion loss is found to be approximately equal to zero. The obtained results can easily prove the powerful and effectiveness of the ECFO-NM algorithm.

It is clear that, the two overlapping ohm Ω figures oriented with their gaps face-to-face are significantly enhanced the matching resonance at the frequency band of 28 GHz. Fig. 5a shows the current distribution of the optimized BPF, which clearly illustrate the high intensity of current distribution at the excited port relative to port 2. On the other side, the maximum electric field intensity is located at the center point within the DGS resonating slots as shown in Fig. 5b. In order to effectively tune the bandpass filter frequency, lumped elements should be placed in appropriate positions within the DGS resonating slots which can be modelled by a parallel LC resonant circuit. Therefore, the capacitors will be placed at the center point of *x*-shape DGS slots.

Fig. 6 illustrates the measured and simulated comparison results of the filter *S*-parameters using CST-MWS and FDTD. As shown in Fig. 6a, it is clear that the designed BP filter can achieve a good impedance matching with S_{11} less than −25 dB at any of the tuned frequency bands. The figure shows the tuning capability of the BP filter over a wide operating band of 4 GHz covering continuous bands from 24 to 28 GHz. Fig. 6c shows the insertion loss of the optimized BP filter at differed tuned frequencies which is found to be less than −2 dB.

B. FILTENNA PERFORMANCE RESULTS

The filtenna is stimulated and optimized to resonate at 28 GHz with minimum axial ratio (*AR*) and high gain (*G*)

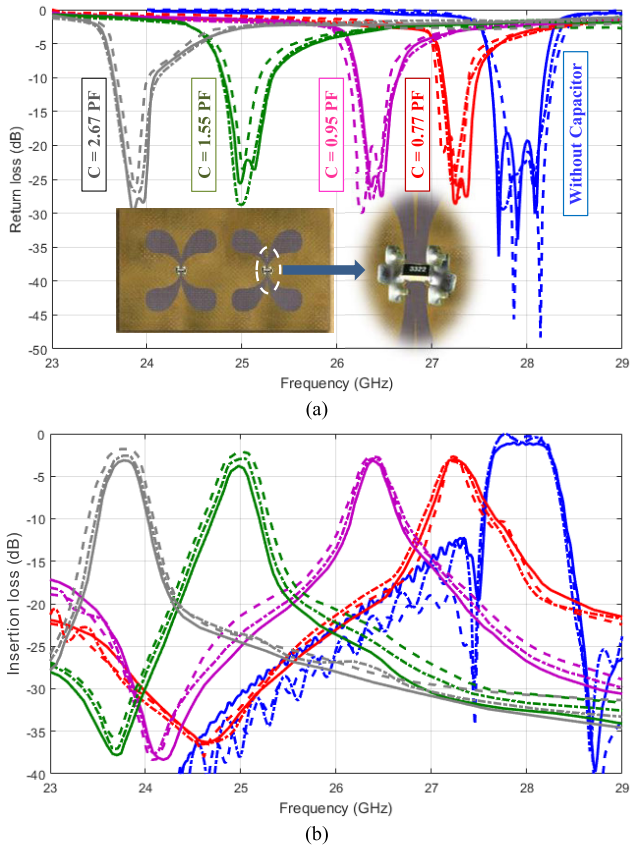

FIGURE 6. S-parameters of the tunable bandpass filter. (a) Return loss and (b) Insertion loss. Solid line (measured), dash-dot line (CST simulation), and dash line (FDTD simulation).

based on the following objective function.

$$Obj_1 = \{min\,[S_{11}] + max\,[G] + min[AR]\}_{f=28GHz} \quad (2)$$

The optimized filtenna dimensions are illustrated in Table 2. Fig. 7a shows the current distribution on filtenna metal parts. It can be noticed that, the current distribution is more concentrated at microstrip feed line and tapered annular radiated patch. This indicates the strength of the mutual coupling effect between the two overlapping omega Ω shape and tapered annular part in filtenna. Moreover, the current distribution in ground plane is more concentrated under the feed line and around the trapezoid gaps g_1 and g_2, otherwise less concentrated current is distributed through other parts of ground plane.

In order to control the filtenna resonance frequency, lumped elements should be placed in appropriate positions within the DGS resonating slots which can be modelled by a parallel LC resonant circuit. Therefore, the position of adding lumped capacitors has been investigated using the CST-MWS simulator. It is found that, the position of maximum electric field intensity within the DGS resonating slots (the longest rib in the trapezoid) shown in Fig. 7b is the best position. Therefore, the capacitors are placed within the center of the

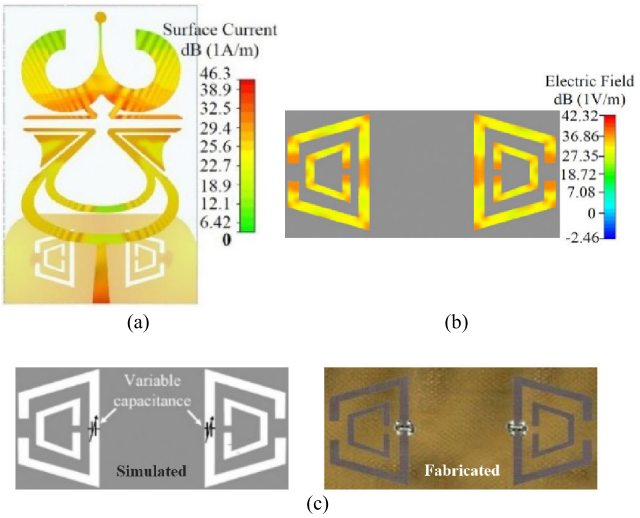

FIGURE 7. Simulated current distribution and electric field intensity of proposed filtenna, (a) Current distribution on filtenna metal parts, (b) Electric field intensity on etched trapezoidal DGS, and (c) Tunable elements position within the DGS resonating slots.

TABLE 2. The filtenna optimized dimensions (in millimeter).

Variable	Initial value	Decision space		Best value
		from	to	
L_5	4	4	7	4.15
L_6	1.5	1.5	4.5	1.65
L_7	1	1	1.5	1.17
L_8	2	2	4	2.55
L_9	1.5	1.5	3.5	2.52
L_c	-	-	-	2
W_4	0.3	0.3	0.65	0.51
W_5	1.5	1.5	2	1.7
W_6	0.8	0.8	1	0.95
W_7	-	-	-	6
W_c	-	-	-	1.5
S_7	0.2	0.2	0.5	0.25
S_8	0.2	0.2	0.5	0.21
R_6	0.5	0.5	1.5	1.09
R_7	1.5	1.5	2.5	2.18
R_8	-	-	-	1.65
R_c	-	-	-	1
g_1	0.1	0.1	0.5	0.125
g_2	0.1	0.1	0.5	0.475

DGS slots as illustrated in Fig. 7c to have a strong effect on the filtenna resonance frequency.

Figs. 8a and 8b illustrate the measured and simulated comparison results of the return loss S_{11} and maximum realized gain, respectively, using CST-MWS and FDTD. It can be observed that, the designed filtenna can achieve a good impedance matching with S_{11} less than -25 dB and a maximum realized gain higher than 9 dB at any of the tuned frequency bands. The figure shows that, the bandpass bandwidth is slightly decreased by increasing the capacitance value which in turn enhances the quality factor and improving the filtenna stored energy. Fig. 8c shows the filtenna radiation efficiency at different resonance frequencies which on average not less than 90%.

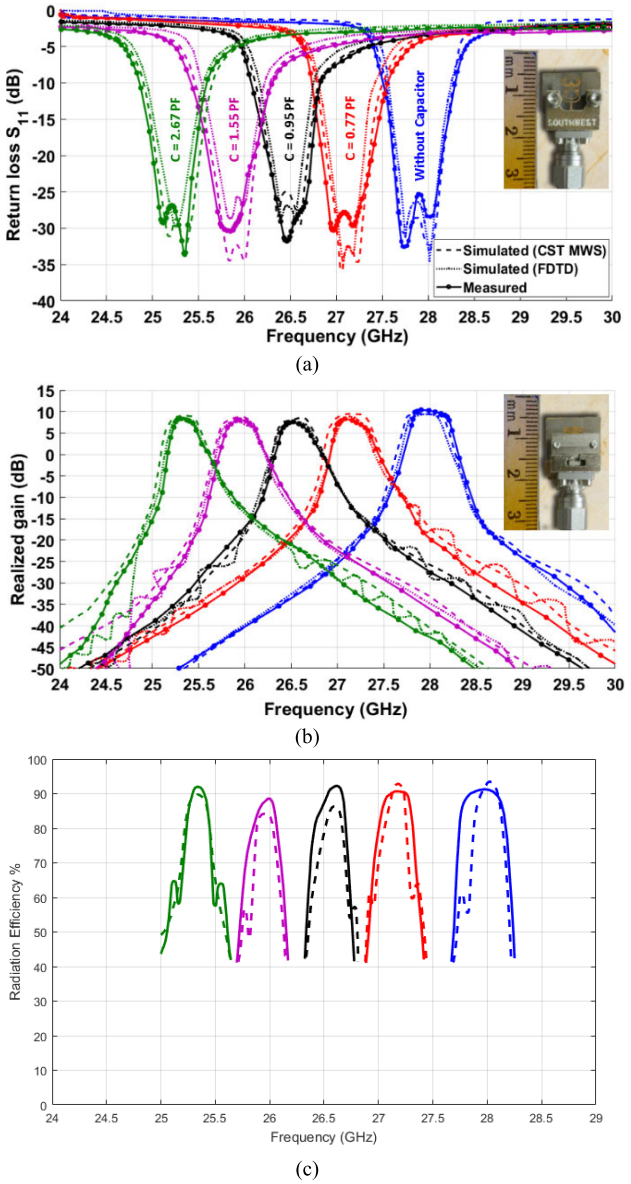

FIGURE 8. Measured and simulated radiation characteristics of proposed filtenna with different capacitor values. (a) Return loss, (b) Realized gain, and (c) Radiation efficiency.

Finally, the 3D radiation pattern of the proposed filtenna at center frequency for each tunable band is shown in Fig. 9. The figure clearly depicts that the filtenna has main radiation direction in the end-fire direction regardless of tuned frequencies. The half power beam-widths in the E-plane at 28, 27.18, 26.61, 25.9, and 25.3 GHz are found to be 88.6°, 92.4°, 89.1°, 87.5°, and 90.7°, respectively, and those in the H-plane to be 73.2°, 77.6°, 75.8°, 70.9°, and 79.3°, respectively. Furthermore, a maximum variation of 0.65 dB in the antenna gain is obtained between the span of capacitance values from 0 to 2.67 PF. These obtained results refer to the radiation characteristic stability of the proposed tuned filtenna at different frequency bands.

It is observed herein that, the strong inductive coupling between the two overlapping omega Ω shape and the tapered

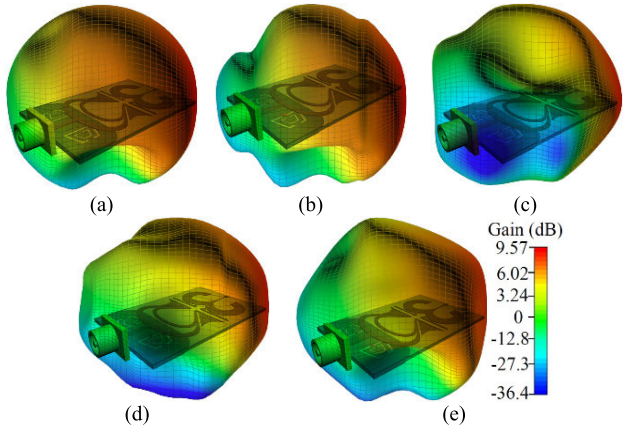

FIGURE 9. 3D field pattern of designed filtenna at different capacitance values. (a) Without capacitance, (b) With C = 0.77 PF, (c) With C = 0.95 PF, (d) With C = 1.55 PF, and (e) With C = 2.67 PF.

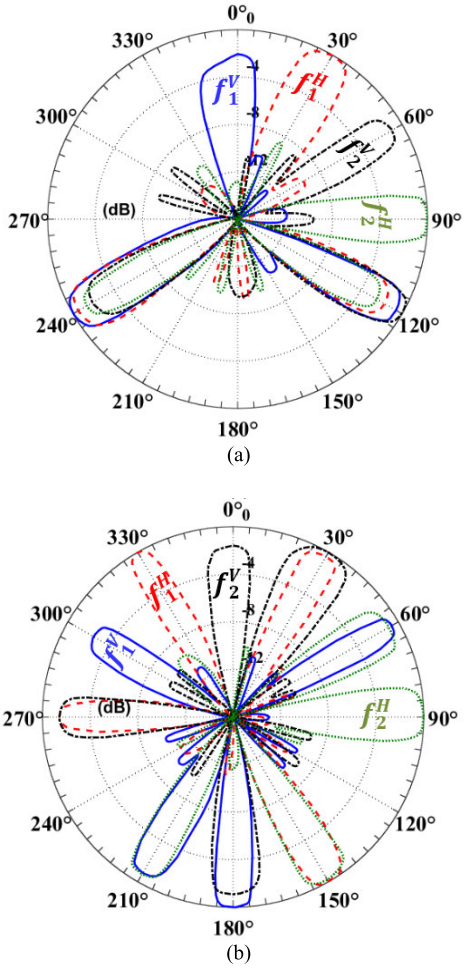

FIGURE 10. The simulation results of 2D radiation patterns of the designed 5G router in x-y plane. (a) Scenario #1 and (b) Scenario #2.

annular radiated patch led to increasing the filtenna gain. Furthermore, the optimized tapered annular radiated patch parameters improved the filtenna matching resonance at different frequency bands. Overall, controlling the overlapping

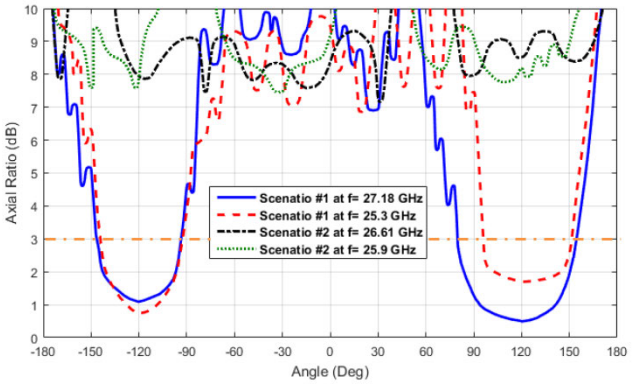

FIGURE 11. Axial ratio of the antenna array versus angels for different scenarios at different frequencies.

omega Ω figures are significantly enhanced the filtenna properties.

C. PERFORMANCE OF mm-wave 5G ROUTER

To synthesize V/H multi-beam patterns adopting polarisation and directivity at two different frequencies simultaneously, the following objective function is used for maximizing the field intensity toward the signal of interest (SOI) and minimizing the output field in the directions of the interfering signals.

$$Obj_3 = \sum_{f=f_1}^{f_2} \left[\sum_{i=1}^{N} |E_\theta(\varphi_i)| + \sum_{j=1}^{M} |E_\varphi(\varphi_j)| - \sum_{k=1}^{P} |E_\theta(\varphi_k)| - \sum_{l=1}^{Q} |E_\varphi(\varphi_l)| \right] \quad (3)$$

where E_φ and E_θ are the horizontal and vertical field intensities, respectively. The constants N and P denotes the number of desired and interferer users, respectively, who will receive V-pol. signals, whereas M and Q symbolize the number of desired and interferer users, respectively, who will be covered with H-pol. signals. In the introduced scenarios, we assumed $N = M = P = Q = 3$ in scenario #1, while in scenario #2, $N = M = 4$, and the number of interferer users $P = Q = 3$.

Figs. 10a and 10b illustrate the optimized beam patterns of the proposed 5G mm-wave router for scenario #1 and scenario #2, respectively. Whereas, the assumed frequencies for scenario #1 were selected to be $f_1 = 27.18$ GHz, and $f_2 = 25.3$ GHz while the other two frequencies $f_1 = 26.61$, and $f_2 = 25.9$ GHz were set for scenario #2. The figure indicates the capability of the proposed filtenna array to maximize the field E_θ and/or E_φ towards the desired directions while placing deeper nulls towards the unwanted directions with two different frequencies simultaneously. Additionally, Fig. 10 show the array capability to serve four users at the same time in the same direction as ensued in scenario #1 at $\varphi = 120°$ and 240° but with different polarizations (either vertical or horizontal) and frequencies (either f_1 or f_2).

Fig. 11 depicts the axial ratio of the filtenna array embedded into router case versus angels for the two scenarios. It is

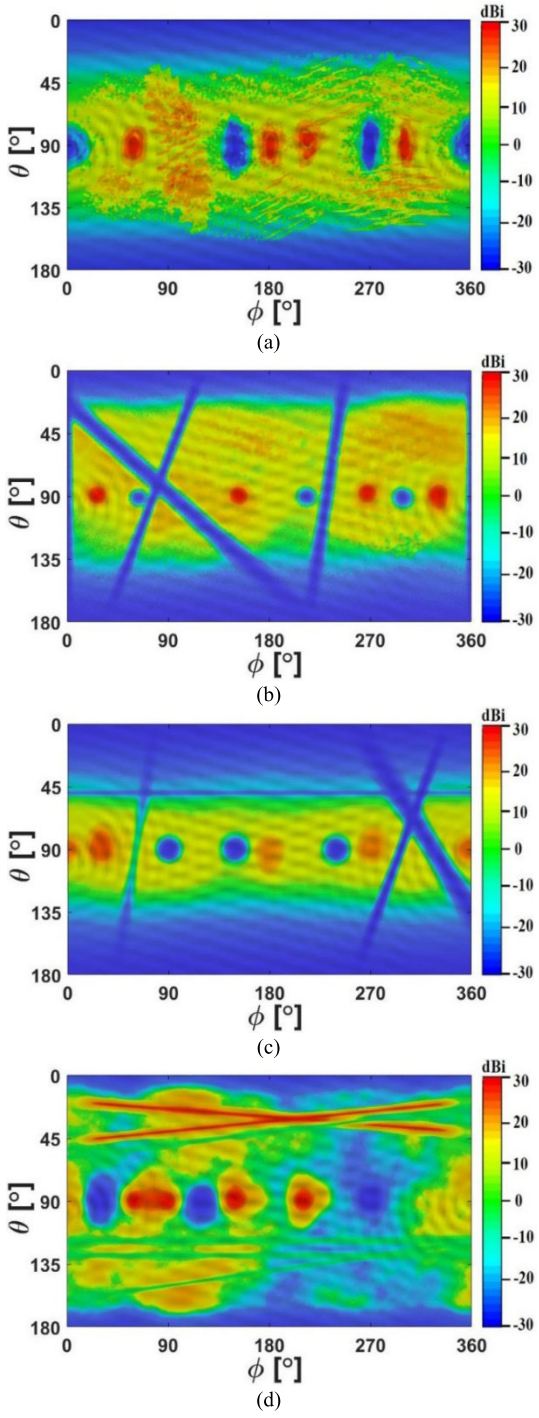

FIGURE 12. Total scan patterns of E_θ and E_φ for scenario #2. (a) At $f_1 = 26.61$ GHz E_θ, (b) At $f_1 = 26.61$GHz E_φ, (c) At $f_2 = 25.9$ GHz E_θ, and (d) At $f_2 = 25.9$ GHz E_φ.

clear that, the proposed 5G router can serve as multi-polarized device, whereas, it can radiate V/H pol. signals in certain directions and as CP in other directions based on the users requirements. As it shown in the figure, the AR is found to be less than 3dB at $\varphi = 60°$ and 240° for scenario #1, whereas four users are located at the same position (two of them is covered with V-pol. beams but with different frequencies

TABLE 3. Descriptions of the environmental scenarios.

			Desired directions			Interferences' directions		
			φ_1	φ_2	φ_3	φ_1'	φ_2'	φ_3'
Scenario #1	f_1 = 27.18 GHz at C = 0.77 pF	V	0°	120°	240°	60°	180°	300°
		H	30°	120°	240°	0°	90°	270°
	f_2 = 25.3 GHz at C = 2.67 pF	V	60°	120°	240°	30°	150°	330°
		H	90°	120°	240°	60°	210°	300°

			Desired directions				Interferences' directions		
			φ_1	φ_2	φ_3	φ_4	φ_1'	φ_2'	φ_3'
Scenario #2	f_1 = 26.61GHz at C = 0.95 pF	V	60°	180°	210°	300°	0°	150°	270°
		H	30°	150°	270°	330°	60°	210°	300°
	f_2 = 25.9 GHz at C = 1.55 pF	V	0°	30°	180°	270°	90°	150°	240°
		H	60°	90°	150°	210°	30°	120°	270°

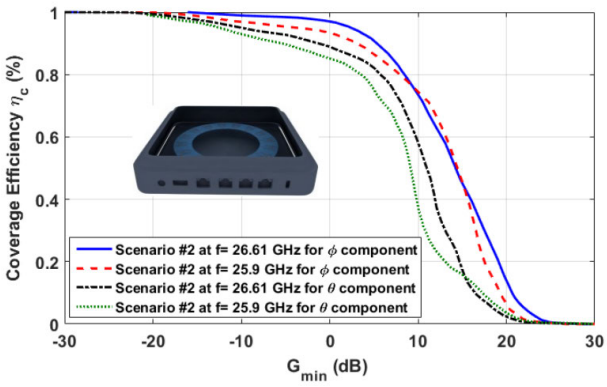

FIGURE 13. Coverage efficiencies comparison of φ and θ-components at different frequencies for scenario #2.

and the others with H-pol. beam patterns each with different frequencies).

To deeply investigate the performance of the mm-wave 5G router, the total scan pattern and coverage efficiency are studied [25], [26]. Whereas, the total scan pattern can be obtained easily by extracting the best attainable gain at every point (θ, φ) from all array patterns corresponding to the electronically steered beams at different feeding phases. Fig. 12 shows the total scan patterns of E_θ and E_φ components, respectively, corresponding to scenario #2 for the designed 5G router device at 26.61 and 25.9 GHz. The obtained total scan patterns clearly illustrate cold spots at the interferer angles and hot spots at desired directions as supposed in Table 3 for both components of E_θ and E_φ at different frequencies.

Based on the calculated total scan pattern, the coverage efficiency (η_c) can be computed as the ratio between the coverage area and the total area [27]. Whereas, the coverage area is defined as the total scan pattern coverage relative to a minimum received gain (G_{min}) and the total area includes the whole surrounding sphere. Fig. 13 show the corresponding η_c as a function of G_{min} for the proposed 5G router at different frequency bands of 27.18, 25.3, 26.61, and 25.9 GHz for two scenarios. It is found that, the coverage efficiency has fallen to 91.64%, and 86.8% when G_{min} exceeds 5 dBi for φ-component, and reduced to 81.94%, and 76.12% for θ-component. These results confirm the applicability of the proposed 5G mm-wave router due to its high coverage efficiency at both frequency bands with different polarizations simultaneously.

IV. CONCLUSION

In this paper, a compact mm-wave tunable DGS bandpass filter, filtenna, and 5G mm-wave router are introduced for future 5G communications. In this target, lumped capacitors have been added within the DGS resonating slots of the filter and filtenna ground plane structure. The optimized filtenna achieved a return loss less than −25 dB with a maximum realized gain higher than 9 dB at any tuned frequency band. Finally, a good agreement has been achieved between measurements and simulated results those produced from the FDTD-Matlab code and CST-MWS. The proposed array design shows the alibility to synthesize multiple V/H directional beams adopting the polarization and directivity control with two different frequencies simultaneously. The promising results show the superior performance of the 5G mm-wave router in terms of gain, return loss, and coverage efficiency.

REFERENCES

[1] Accessed: Jul. 2019. [Online]. Available: https://www.sdxcentral.com/5g/definitions/5g-router-future-connectivity/
[2] (Jul. 2019). *GSMA Public Policy Position-5G Spectrum*. [Online]. Available: https://www.com
[3] Accessed: Jul. 2019. [Online]. Available: https://venturebeat.com/2018/05/01/samsung-5g-home-router-wins-fcc-approval-ahead-of-verizons-2018-launch/
[4] M. Mandal and Z. Chen, "Compact wideband coplanar stripline bandpass filter with wide upper stopband and its application to antennas," *IET Microw. Antennas Propag.*, vol. 4, no. 12, p. 2166, 2010.
[5] Y. Sung, "Triple band-notched UWB planar monopole antenna using a modified H-shaped resonator," *IEEE Trans. Antennas Propag.*, vol. 61, no. 2, pp. 953–957, Feb. 2013.
[6] J. Y. Siddiqui, C. Saha, and Y. M. M. Antar, "Compact SRR loaded UWB circular monopole antenna with frequency notch characteristics," *IEEE Trans. Antennas Propag.*, vol. 62, no. 8, pp. 4015–4020, Aug. 2014.
[7] C. Lin, P. Jin, and R. Ziolkowski, "Single, dual and tri-bandnotched UWB antennas using CLL resonators," *IEEE Trans. Antennas Propag.*, vol. 60, no. 1, pp. 102–109, 2012.
[8] J. Zuo, X. Chen, G. Han, L. Li, and W. Zhang, "An integrated approach to RF antenna-filter Co-design," *IEEE Antennas Wireless Propag. Lett.*, vol. 8, pp. 141–144, 2009.
[9] S. Ranjan Mishra, K. L. Sheeja, and N. P. Pathak, "Split ring resonator inspired microstrip filtenna for Ku-band application," *J. Eur. des Syst. Autom.*, vol. 50, nos. 4–6, pp. 391–403, Dec. 2017.
[10] M.-C. Tang, Y. Wang, and Y. Chen, "Design of compact filtennas with enhanced bandwidth," in *Proc. IEEE Int. Conf. Signal Process., Commun. Comput. (ICSPCC)*, Sep. 2018, pp. 1–4.
[11] N. Miswadi, M. Ali, M. Tan, and F. Redzwan, "Design of filtenna with bandstop element for Ultra-Wideband (UWB) applications," in *Proc. Int. Conf. Comput., Commun., Control Technol. (ICT)*, Apr. 2015, pp. 21–23.

[12] S. R. Mishra and S. K. Lalitha, "Filtennas for wireless application: A review," *Int. J. RF Microw. Comput.-Aided Eng.*, vol. 29, no. 10, Oct. 2019, Art. no. e21879.
[13] M.-C. Tang, Y. Wang, Y. Chen, and R. W. Ziolkowski, "Designs of compact, planar, wideband, monopole filtennas with near-field resonant parasitic elements," in *Proc. IEEE Int. Conf. Comput. Electromagn. (ICCEM)*, Mar. 2018, pp. 26–28.
[14] C. Yu and W. Hong, "37-38 GHz substrate integrated filtenna for wireless communication application," *Microw. Opt. Technol. Lett.*, vol. 54, no. 2, pp. 346–351, Feb. 2012.
[15] M. M. Hosain, S. Kumari, and A. K. Tiwary, "Compact filtenna for WLAN applications," *J. Microw. Optoelectron. Electromagn. Appl.*, vol. 18, no. 1, pp. 70–79, Mar. 2019.
[16] C.-J. Wang and C.-S. Lin, "Compact DGS resonator with improvement of Q-factor," *Electron. Lett.*, vol. 44, no. 15, p. 908, 2008.
[17] K. R. Mahmoud and A. M. Montaser, "Optimised 4×4 millimetre-wave antenna array with DGS using hybrid ECFO-NM algorithm for 5G mobile networks," *IET Microw., Antennas Propag.*, vol. 11, no. 11, pp. 1516–1523, 2017.
[18] I. F. da Costa, "Optically controlled reconfigurable antenna for 5G future broadband cellular communication networks," *J. Microw., Optoelectron. Electromagn. Appl.*, vol. 16, no. 1, pp. 208–217, 2017.
[19] J. T. Bernhard, "Reconfigurable antennas," in *Encyclopedia of RF and Microwave Engineering*, K. Chang, Ed., New York, NY, USA: Wiley, 2005.
[20] A. Boukarkar, "Compact mechanically frequency and pattern reconfigurable patch antenna," *IET Microw., Antennas Propag.*, vol. 12, no. 11, pp. 1864–1869, 2018.
[21] L. Safatly, M. Bkassiny, M. Al-Husseini, and A. El-Hajj, "Cognitive radio transceivers: RF, spectrum sensing, and learning algorithms review," *Int. J. Antennas Propag.*, vol. 2014, Mar. 2014, Art. no. 548473.
[22] H. A. Atallah, K. Yoshitomi, A. B. Abdel-Rahman, and R. K. Pokharel, "Compact frequency reconfigurable filtennas using varactor loaded T-shaped and H-shaped resonators for cognitive radio applications," *IET Microw., Antennas Propag.*, vol. 10, no. 9, pp. 991–1001, Jun. 2016.
[23] A. A. C. Alves, L. G. Da Silva, E. C. Vilas Boas, D. H. Spadoti, and S. Arismar Cerqueira, "Continuously frequency-tunable horn filtennas based on dual-post resonators," *Int. J. Antennas Propag.*, vol. 2019, pp. 1–12, Sep. 2019.
[24] K. R. Mahmoud, "Synthesis of unequally-spaced linear array using modified central force optimisation algorithm," *IET Microw., Antennas Propag.*, vol. 10, no. 10, pp. 1011–1021, Jul. 2016.
[25] K. R. Mahmoud and A. M. Montaser, "Synthesis of multi-polarised upside conical frustum array antenna for 5G mm-Wave base station at 28/38 GHz," *IET Microw., Antennas Propag.*, vol. 12, no. 9, pp. 1559–1569, Jul. 2018.
[26] K. R. Mahmoud and A. M. Montaser, "Performance of tri-band multi-polarized array antenna for 5G mobile base station adopting polarization and directivity control," *IEEE Access*, vol. 6, pp. 8682–8694, 2018.
[27] J. Helander, D. Sjoberg, M. Gustafsson, K. Zhao, and Z. Ying, "Characterization of millimeter wave phased array antennas in mobile terminal for 5G mobile system," in *Proc. IEEE Int. Symp. Antennas Propag. USNC/URSI Nat. Radio Sci. Meeting*, Vancouver, BC, Canada, Jul. 2015, pp. 7–8.

KORANY R. MAHMOUD received the B.S. and M.S. degrees in communications and electronics engineering from Helwan University, in 1998 and 2003, respectively, and the Ph.D. degree from Helwan University in collaboration with the University of Connecticut, USA, in 2008. He is currently a Professor with the Department of Communications and Electronics Engineering, Helwan University. He is also the Vice Dean of the Community Service and Environmental Development. Since 2012, he served as a Consultant for the Research and Development Department, National Telecommunications Regulatory Authority (NTRA), Egypt. He has also been working as a Postdoctoral Fellow at the CPSM Center (Center for Photonics and Smart Materials), Zewail City, Egypt. He has published over 65 refereed journal and conference papers in addition to one book on reconfigurable microwave filter. His current research interests include the areas of 5G mm-wave and optical nano-antennas design for modern wireless applications using metaheuristic optimization techniques, as well as microwave filters design and radar cross section reduction techniques.

AHMED M. MONTASER received the B.S. and M.S. degrees in communications and electronics engineering from South Valley University, Aswan, Egypt, in 2003 and 2009, respectively, and the Ph.D. degree from Mansoura University, Egypt, in 2013. He is currently an Associate Professor with the Department of Communication and Electronics, Sohag University, Sohag, Egypt. He has authored more than 27 articles on microwave based smart antenna, conformal array devices, and mmWave antennas. He has served as an editor/reviewer for many international journals. His current research interests include the areas of microwave applications in biomedical, especially in breast and brain cancer, hyperthermia, and using millimeter wave for cancer detection.